

## Ni-Cr Layered Double Hydroxide/Microcrystalline Cellulose Composite as Adsorbents for Malachite Green Dye

Rotua Natalia Manalu<sup>1</sup>, Zaqiya Artha Zahara<sup>2</sup>, Risfidian Mohadi<sup>3\*</sup>

<sup>1</sup>Research Center of Inorganic Materials and Coordination Complexes, Universitas Sriwijaya, Palembang, South Sumatera, 30139, Indonesia

<sup>2</sup>Magister Programme in Environment Management, Sriwijaya University, Palembang, South Sumatera, 30139, Indonesia

<sup>3</sup>Graduate School, Faculty of Mathematics and Natural Sciences, Sriwijaya University, Jl. Palembang-Prabumulih, Km. 32, Ogan Ilir, 30862, Indonesia

\*Corresponding author: risfidian.mohadi@unsri.ac.id

### Abstract

Malachite green dye in industrial wastewater can be removed by the adsorption method. The adsorbents used in the adsorption method were Ni-Cr LDH, microcrystalline cellulose, and Ni-Cr LDH/microcrystalline cellulose composite. Regeneration process of malachite green dye with the Ni-Cr/microcrystalline cellulose adsorbent resulted in the adsorbent having the highest percent adsorbed when compared to Ni-Cr LDH and microcrystalline cellulose adsorbents. This is proof that Ni-Cr/microcrystalline cellulose LDH composite adsorbent can be used repeatedly as much as five cycles. Ni-Cr LDH material and Ni-Cr/microcrystalline cellulose LDH composite were synthesized by the coprecipitation method and were successfully carried out by XRD characterization to see the stability of the structure. The results of XRD characterization of Ni-Cr/microcrystalline cellulose composite showed peaks at diffraction angles of  $11^\circ(003)$ , and  $60^\circ(110)$  which are typical regions of LDH and at diffraction angle of  $22^\circ(020)$  which is a typical area of microcrystalline cellulose material. Ni-Cr LDH, microcrystalline cellulose and Ni-Cr/microcrystalline cellulose get optimum pH at 7 with wavelength malachite green at 618.8 nm, kinetic equation following PSO and isotherm following Freundlich with capacity maximum until  $129.870 \text{ mg.g}^{-1}$ . FT-IR spectra display groups found in LDH and composites including O-H,  $\text{NO}_3^-$ , M-O also microcrystalline cellulose have groups C-O and C-H. SEM characterization found out the biggest particle size is  $1,954 \mu\text{m}$  as much as 72 and EDX composite material contains elements of O, C, Ni, Cr, Na, and N.

### Keywords

Malachite Green, Layered Double Hydroxide, Microcrystalline Cellulose, Adsorption

Received: 3 May 2023, Accepted: 13 July 2023

<https://doi.org/10.26554/ijmr.2023128>

## 1. INTRODUCTION

A major problem faced by developing countries is environmental pollution that impacts the economy through untreated dye effluents from the textile industry (Olisah et al., 2021). Based on the data obtained by (Chandanshive et al., 2020), each year  $7 \times 10^7$  tonnes of textile dyes are produced and more than 10,000 dyes are used for industrial textiles. There are several basic types of industrial dyestuffs, which are also classified into chemical structures and applications (Al-Tohamy et al., 2022). Dyes found throughout the textile industry include azo, acid, bases, direct dyes, reactive dyes, dispersions, sulfides and mordants (Silva et al., 2021). One of the most popular dyes known in the textile industry is malachite green. Malachite green is a slightly blackish - coloured and as cationic dyes with a chemical structure  $\text{C}_{23}\text{H}_{25}\text{ClN}_2$  and an assigned molecular weight of  $364.9 \text{ g/mol}$  (Ahmed et al., 2022). A complex structure, highly resistant to oxidising agents, and has a high stability that makes malachite

green dyes challenging to decompose naturally (Hamad and Moustafa, 2023). Ingestion of malachite green has been banned in many USA and European countries primarily due to the carcinogenicity of malachite green, which is harmful to aquatic life such as animals and microorganisms, and the W.H.O considers malachite green to be a Class III of hazardous dyes (Sinha and Jindal, 2018). Malachite Green also has genotoxic properties that are harmful to humans, when consuming foods containing this dye, liver tumours are one of the diseases that will appear (Matpang et al., 2017).

Government standards for the discharge of dyes into waters have been set, thus requiring the treatment before dyes released into water. Substance dyes removal methods are separated in three categories, which are biological, chemical, and physical treatment (Tang et al., 2018), hopefully developing methods that can treat dye waste and can be reused (Sarro et al., 2018). Methods of treating dye effluent include algae degradation (Adegoke and Bello, 2015), ozonation (Venkatesh et al., 2017), photochem-

ical (Dang et al., 2016), coagulation and flocculation (Karam et al., 2021), ion exchange (Nandoost et al., 2022), reverse osmosis (Abid et al., 2012), membrane filtration (Ashraf et al., 2019), also adsorption. Adsorption has been used as a treatment for malachite green dye via the pore absorption mechanism of the adsorbent for the dye (liquid-solid), but the adsorption process is also possible to be carried out in phases liquid-liquid, gas-liquid, gas-solid (De Gisi et al., 2016). Adsorption process is broadly divided into two types, chemically and physically, and can be undertaken on an industrial or laboratory scale. Parameters that affect adsorption include pH, contact time of adsorbent and adsorbate, solution temperature, as well as adsorbent weight and dye concentration (Ballav et al., 2018). Another advantage in using the adsorption method is that easy, non-reactive process, inexpensive equipment, and adsorbents can be used repeatedly (Katheresan et al., 2018).

Researchers have developed many adsorbents consisting of activated carbon (Sartape et al., 2017), chitosan, metal oxide-based compounds (Muinde et al., 2020), natural clay (Venkatesh et al., 2017), hematite iron oxide nanoparticle (Dehbi et al., 2020), and layered double hydroxide (LDH) (Palapa et al., 2022). Layered double hydroxide on the other is also known as an anionic hydroxalite or clay (Correcher and García-Guinea, 2018). The use of LDH has been extensively developed in the fields of catalysts, electrode/conductor materials, batteries, and hydrogen (H<sub>2</sub>) and oxygen (O<sub>2</sub>) production (Gomes et al., 2016), ion exchangers and adsorbents were are characterized by the following general formula  $[M^{2+}_1 - xM^{3+}_x(OH)_2]_x^+ [An^{-x}/n.mH_2O]$  where M<sup>2+</sup> (Ni, Zn, Mg) and M<sup>3+</sup> (Al, Cr, Fe) are metal valences, x is the molar ratio and An<sup>-</sup> is the anion in the layer (Palapa et al., 2022). An important characteristic of layered double hydroxides is the flexibility through which the anions in the interlayer are switchable and have intercalation process depending to the application of the layered double hydroxide (Taher et al., 2019). Some of the interchangeable anions is oxalate anion (Doungmo et al., 2016), which is intended to promote interlayer spacing. In addition to these advantages, LDH is made at low cost, has good chemical stability. One disadvantage of LDH is that it cannot be used repeatedly so modification with carbon material is required (Ashkuzzaman and Jiang, 2014). Microcrystalline cellulose was favoured for modification with LDH as it has thermally stable, biocompatible, and can be applied in adsorption processes (Fouad et al., 2020).

Based on the modification of Mg-Cr LDH with microcrystalline cellulose conducted by Yuliasari et al. (2023) for removing phenol, it was found that the maximum capacity reached 58.480 mg.g<sup>-1</sup> compared to Mg-Cr LDH which only reached 24,631 mg.g<sup>-1</sup> by following the Langmuir constant and Mg-Cr/microcrystalline cellulose can be regenerated five cycles. Jiang et al. (2022) project on methyl orange dye adsorption kinetics of Ni-Cr LDH-FA-W achieved equilibrium at 2 hours time which followed PSO kinetics, the isotherm of adsorption measured 806 mg.g<sup>-1</sup> and the thermodynamics of adsorption was endothermic and the reaction was spontaneous. Cationic malachite green dyes treatment using Ni-Al/hydrochar by (Normah

et al., 2021) with adsorption capacity up to 256,410 mg.g<sup>-1</sup> and Ni-Al/hydrochar adsorbent can be used 7 times.

The experiment was started to prepare adsorbent layered double hydroxide composites using cellulose microcrystalline. Adsorbents applied to remove malachite green from aqueous solution. Adsorbents were characterized by XRD analysis to identify the phase of the material. Infra-red spectrophotometer analysis to identify the presence of functional groups present in the material. SEM analysis aims to analyse morphology. In this study, there are factors that affect the adsorption process, namely the effect of pH, the effect of adsorption time, the effect of concentration, and adsorption temperature. Ni-Cr/microcrystalline cellulose LDH composite was analysed for repeated applications of the adsorbent.

## 2. EXPERIMENTAL SECTION

### 2.1 Materials

Materials used in the present study include distilled water (H<sub>2</sub>O), hydrochloric acid (HCl), Chromium (III) nitrate nonahydrate (Cr(NO<sub>3</sub>)<sub>3</sub>·9H<sub>2</sub>O), malachite green (C<sub>23</sub>H<sub>25</sub>ClN<sub>2</sub>), sodium hydroxide (NaOH), nickel (II) nitrate hexahydrate (Ni(NO<sub>3</sub>)<sub>2</sub>·6H<sub>2</sub>O) and microcrystalline cellulose (C<sub>6</sub>H<sub>10</sub>O<sub>5</sub>)<sub>n</sub>.

### 2.2 Ni-Cr LDHs Synthesis (Ruan et al., 2016)

Ni-Cr LDH material was carried out by coprecipitation method. Firstly, 100 mL of Ni(NO<sub>3</sub>)<sub>2</sub>·6H<sub>2</sub>O 0.3 M and 100 mL of Cr(NO<sub>3</sub>)<sub>3</sub>·9H<sub>2</sub>O 0.1 M were mixed. Next, 100 mL of 1.0 M NaOH was added until the pH was 8. Temperature was set at 60°C during the addition. Stirring was carried out constantly for 12 hours at a temperature of 80°C. After that, it was cooled for several hours and then filtered and washed using distilled water. The precipitate was dried for 24 hours using an oven at 60°C. Ni-Cr solid was successfully obtained and then crushed until smooth, then characterized using XRD, FTIR and SEM.

### 2.3 Preparation Ni-Cr/microcrystalline Cellulose

Ni(NO<sub>3</sub>)<sub>2</sub>·6H<sub>2</sub>O 0.25 M as much as 30 mL was mixed with Cr(NO<sub>3</sub>)<sub>3</sub>·9H<sub>2</sub>O 0.75 M in 30 mL and then stirred while slowly dropping 2 M NaOH solution until pH 10, stirring was carried out for 1 hour. Then 3 grams of microcrystalline cellulose was added and stirred for 72 hours at 80°C. The solid obtained was filtered and washed with distilled water and then dried in the oven at 100°C after which it was crushed until smooth and obtained Ni-Cr/microcrystalline cellulose LDH composite material. Then characterisation was carried out using XRD, FTIR and SEM.

### 2.4 Regeneration Process

The regeneration process is performed by desorption of malachite green dye adsorbed on the adsorbent with an ultrasonic device. Ni-Cr/microcrystalline cellulose LDH composite is weighed by 0.02 g which has been desorbed with a suitable solvent added to the malachite green at a concentration of 30 mg/L. The complaint was made for 150 minutes and a measurement was made for the absorption value of malachite green. The used adsorbent

is then dried at room temperature and reused for regeneration by repeating five times.

### 2.5 Adsorption Experiment

Ni-Cr LDH, microcrystalline cellulose, and Ni-Cr/microcrystalline cellulose LDH composite as much as 0.02 grams with 20 mL of malachite green dye solution were influenced by pH set in the range of 2-11 using NaOH 0.1 M and HCl 0.1 M, after the optimum pH was obtained, it was used for time variations with variations of 5, 10, 20, 30, 40, 50, 60, 70, 90, 120, 150, 180 and 210 minutes. The effect of concentration and temperature was carried out using the optimum pH and time obtained, where the concentration variations were 30, 40, 50, 60 and 70 mg/L, with temperatures of 30, 40, 50, 60 and 70 °C. The filtrate obtained was measured using a UV-Vis spectrophotometer and the absorbance value was recorded.

## 3. RESULTS AND DISCUSSION

### 3.1 Regeneration Process

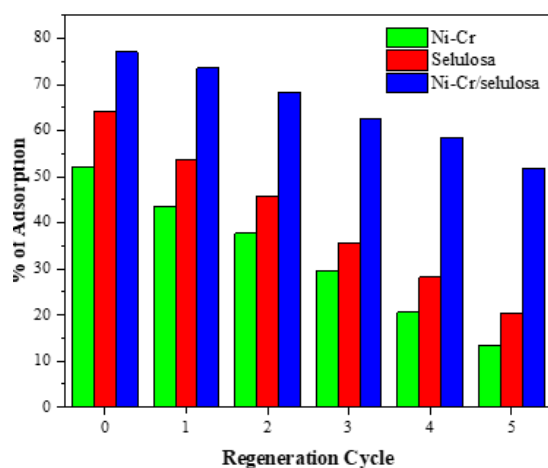


Figure 1. Graphic Regeneration Process

Regeneration is needed in industrial processes to reduce adsorbent manufacturing expenses and create an environmentally friendly adsorbent. The regeneration cycle can determine that there is a percentage decrease in the adsorption of malachite green as the regeneration process increases on each adsorbent retrieved in Figure 1. During the first regeneration, adsorbent Ni-Cr/cellulose microcrystalline had the highest percent adsorbed that is 51.873% at fifth regeneration when compared to the Ni-Cr and cellulose microcrystalline adsorbents which have a sequential percent adsorbed 13.308% and 20,261%. The regeneration process of Ni-Cr LDH and cellulose microcrystalline towards malachite green adsorption process shows that the decrease in percent adsorbed is quite drastic, it can be seen to first until fifth regeneration which shows that the unstable structure of the adsorbent in the regeneration process against malachite green dye. Throughout the regeneration cycle of Ni-Cr/cellulose microcrystalline adsorbent for malachite green dye, there was a

slow decrease in the percent adsorbed. This indicates that the adsorbent has a structure that is quite stable to the regeneration process towards the absorption of malachite green dye. Thus, the Ni-Cr/cellulose microcrystalline adsorbent is more optimally used as an adsorbent for repeated use compared to Ni-Cr LDH and cellulose microcrystalline.

### 3.2 Analyze XRD (X-Ray Diffraction) Characterization

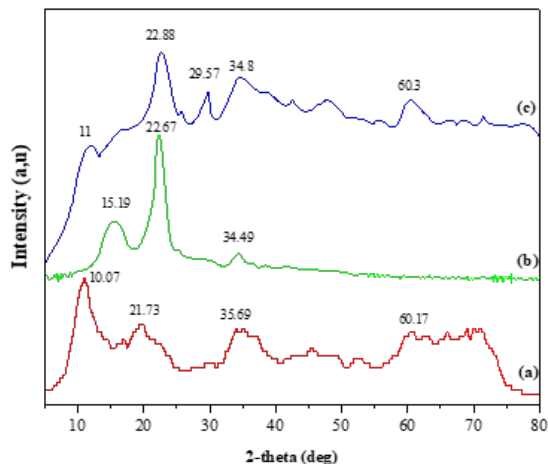


Figure 2. Diffractograms of Ni-Cr (a) Microcrystalline Cellulose (b) and Ni-Cr/microcrystalline Cellulose (c)

Stability or instability of a structure seen from XRD results thus knowing whether the adsorbent is reusable and knowing the typical angle of the adsorbent LDH and cellulose microcrystalline. Diffractogram of Ni-Cr LDH presented in Figure 2(a) shows that there are fractions show the characteristic of Ni-Cr LDH at angles of 7.7° (003), 21.7° (006), 39.6° (009), and 56.1° (110) and in accordance with the data JCPDS No.15-008. Previous research conducted by Ye et al (2018) showed diffraction peaks of Ni-Cr LDH material at 11.4° (003), 23.3° (006), 34° (009), and 60.8° (110). It is typical of materials with a multilayer structure that peaks appear. The XRD characterisation results obtained show that the Ni-Cr LDH material was successfully synthesised. Damaged structure of Ni-Cr LDH can be observed from the shift of diffractogram after adsorbent usage for regeneration.

Microcrystalline cellulose regeneration occurs in amorphous phases from diffractogram XRD, shown in Figure 2(b). Microcrystalline cellulose shows the characteristics of cellulose at diffraction angles of 15.19° (101), 22.67° (002), and 34.49° (004) which the results are amorphous and crystalline. Osman et al. (2022) have conducted research appearing peak with the highest intensity at an angle of 15.1° (101); 22.08° (002); and 34.75° (004). Ni-Cr LDH was modified with carbon-based materials, i.e. microcrystalline cellulose, with the objective of forming a Ni-Cr/microcrystalline cellulose LDH composite adsorbent to enable the resulting adsorbent to be used repeatedly in the adsorption process, so that mechanisms in the regeneration process are known. Composite could be used repeatedly by looking at XRD measurement results after adsorption, indicating that there

**Table 1.** Kinetics Model of Malachite Green Dye Adsorption on Ni-Cr, Microcrystalline Cellulose, and Ni-Cr/microcrystalline Cellulose

Adsorbate	Kinetic Model	Parameter	Ni-Cr	Microcrystalline Cellulose	Ni-Cr/microcrystalline Cellulose
Malachite Green	Pseudo First Order (PFO)	qe eksperiment (mg/g)	15.2380	20.0688	27.7847
		qe calculation (mg/g)	16.2144	23.6919	29.6688
		$k_1$ ( $\text{min}^{-1}$ )	2.7864	3.1657	3.3907
		$R^2$	0.8632	0.8996	0.9601
	Pseudo Second Order (PSO)	qe eksperiment (mg/g)	15.2380	20.0688	27.7847
		qe calculation (mg/g)	15.5674	21.9298	30.1205
		$k_2$ (g/mg.min)	0.0026	0.0020	0.0018
		$R^2$	0.931	0.9742	0.9846

is no change in the porosity of the composite. Diffractogram of the Ni-Cr/microcrystalline cellulose LDH composite in Figure 2(c) depicted that there are fractions exhibiting the characteristics of the Ni-Cr/microcrystalline cellulose LDH composite, namely at angles of  $11^\circ$  (003),  $22.8^\circ$  (002),  $34.8^\circ$  (004), and  $60.3^\circ$  (110). These x-ray diffraction (XRD) characterization results prove that Ni-Cr/microcrystalline cellulose LDH composite has been successfully composited.

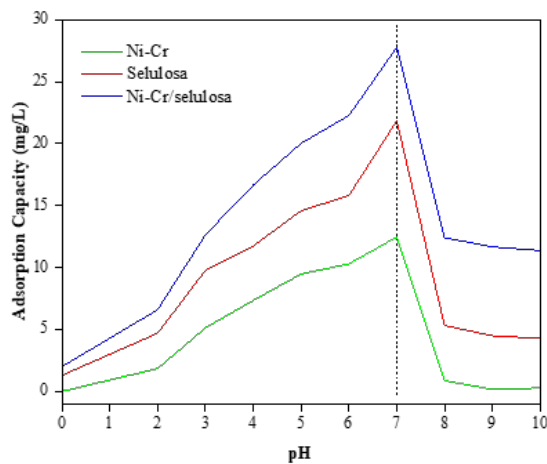


**Figure 3.** Effect of pH Adsorbents on Malachite Green Dye

### 3.3 Adsorption Process

Once established that the adsorbent can be used repeatedly and the characteristic angle of the adsorbent is identified which is intended because the adsorption process occurs on the surface of the adsorbent. Base on the data in Figure 3, optimum pH for adsorption of malachite green dye at pH 7 on adsorbent Ni-Cr, microcrystalline cellulose, and Ni-Cr/microcrystalline cellulose

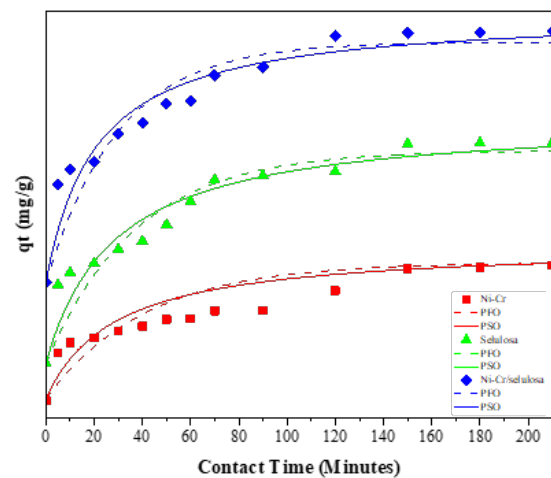


**Figure 4.** Effect of Adsorption Time of Malachite Green Dye on Adsorbents

measured by using the largest adsorption capacity with wavelength at maximum absorbance of 618.8 nm. The results of [Medidi et al. \(2018\)](#) study of the maximum wavelength for malachite green dye is 617 nm. Each of adsorbents Ni-Cr/microcrystalline cellulose, microcrystalline cellulose, and Ni-Cr pH for dye was determined to ensure the optimal adsorption process. [Eltaweil et al. \(2020\)](#) reported that at acidic pH, the addition of  $\text{H}^+$  ion concentration causes the adsorption process to not run optimally, because the addition of positively charged ions on the surface of the adsorbent results in repulsion between the adsorbent and malachite green which has cationic properties. Neutral pH causes the adsorption to run optimally because the negative charge of  $\text{OH}^-$  ions on the adsorbent surface increases, resulting in an electrostatic attraction force between the adsorbent and

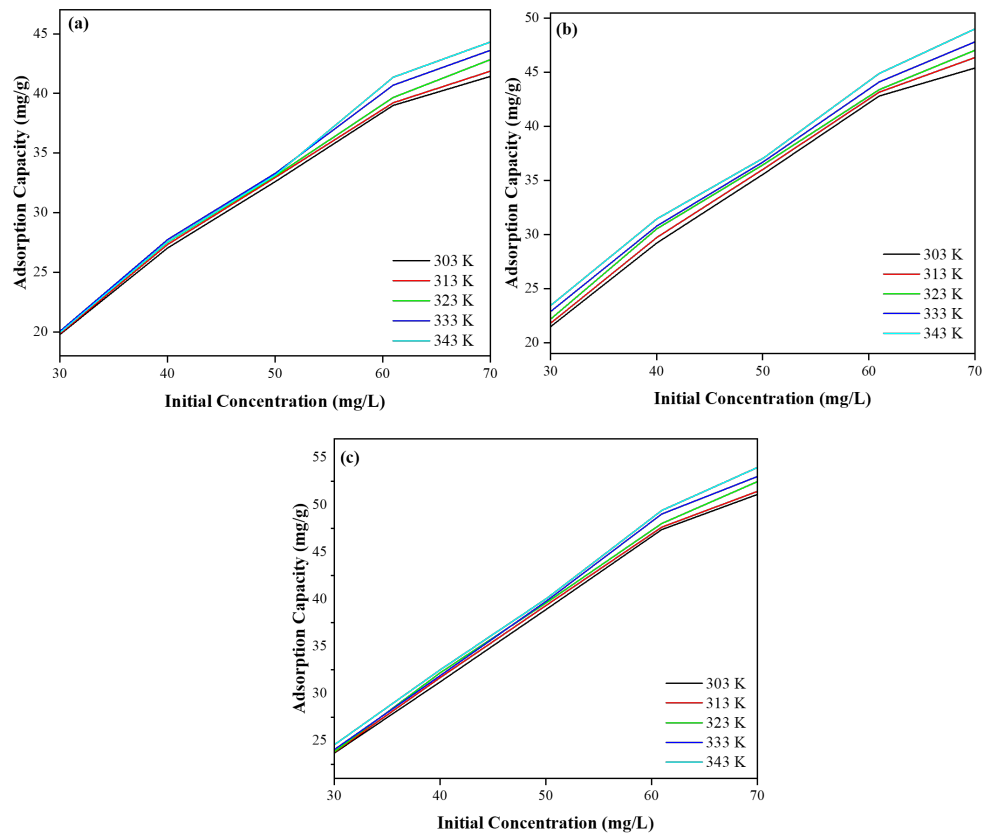


**Figure 5.** Influence of Concentration and Temperature of Ni-Cr (a) Microcrystalline Cellulose (b) and Ni-Cr/microcrystalline Cellulose (c)

the malachite green dye. While at the alkaline pH, adsorption does not work optimally because malachite green dye undergoes deprotonation which causes changes in the structure of the dye. Malachite green in highly acidic conditions will be protonated due to excess  $H^+$  ions and in highly alkaline conditions will be deprotonated due to excess  $OH^-$  ions.

Figure 4 illustrates the impact of time on adsorption capacity. The results demonstrate that equilibrium was attained at 150 minutes, indicating a constant adsorption concentration for each adsorbent, namely Ni-Cr LDH, microcrystalline cellulose, and Ni-Cr/microcrystalline cellulose. Table 1 provides data on the pseudo first-order (PFO) and pseudo second-order (PSO) kinetics models for malachite green on these adsorbents. By examining the effect of adsorption time on malachite green dye, the adsorption rates can be determined using PFO and PSO kinetics. The kinetics model enables the establishment of the adsorption process by evaluating the coefficient of determination ( $R^2$ ) value close to 1 and the resemblance between the experimental  $Q_e$  value and the calculated  $Q_e$ . These parameters are indicative of the maximum adsorption capacity of an adsorbent in terms of adsorption kinetics. Imbalances in the kinetic process are expressed in the form of differential equations to model the kinetics of PFO, generally due to the physics of the adsorption process, whereas PSO is better used to describe experimental data and adsorption

processes occur chemically (Guo and Wang, 2019). Based on the kinetic data obtained when determining the adsorption rate, Ni-Cr, microcrystalline cellulose, and Ni-Cr/microcrystalline cellulose are closer to the pseudo second order kinetic model. The value of the coefficient of determination ( $R^2$ ) is close to 1 and the experimental  $Q_e$  value in the PSO kinetic model is closer to the calculated  $Q_e$ .

According to the graphs in Figure 5, the relationship between the temperature and concentration of malachite green dye indicates a direct proportionality to the increase in adsorption capacity. As the concentration and temperature of malachite green dye increased, the adsorption capacity also increased. The highest adsorption capacity was observed when the initial concentration of malachite green dye was 70 mg/L at a temperature of 70°C. The Ni-Cr/microcrystalline cellulose LDH composite adsorbent exhibited the highest capacity at 57.855 mg/L, followed by microcrystalline cellulose at 52.422 mg/L, and Ni-Cr LDH at 49.230 mg/L. Therefore, it is evident that incorporating microcrystalline cellulose, a carbon-based material, into LDH resulted in a significantly enhanced adsorption capacity.

Data in Table 2 proves that the adsorption process of malachite green dye using composite adsorbents of ldh Ni-Cr/cellulose, cellulose, and ldh Ni-Cr is likely to approach the Freundlich isotherm model. Moreover, the linear regression coefficient value

**Table 2.** Isotherm Model for Removal Malachite Green Use Ni-Cr, Microcrystalline Cellulose, and Ni-Cr/microcrystalline Cellulose

Adsorbents	Adsorption Isotherm	Adsorption Constant	T (K)				
			30°C	40°C	50°C	60°C	70°C
Ni/Cr	Langmuir	Qmax	100.000	87.719	84.034	80.645	85.470
		kL	0.027	0.038	0.048	0.062	0.069
		R <sup>2</sup>	0.833	0.909	0.956	0.964	0.950
	Freundlich	n	1.400	1.536	1.628	1.733	1.721
		kF	4.070	5.351	6.519	7.991	8.929
		R <sup>2</sup>	0.944	0.943	0.96	0.958	0.955
Microcrystalline Cellulose	Langmuir	Qmax	104.167	87.719	87.719	90.909	92.593
		kL	0.034	0.053	0.060	0.065	0.076
		R <sup>2</sup>	0.827	0.947	0.933	0.954	0.947
	Freundlich	n	1.422	1.619	1.667	1.660	1.710
		kF	5.199	7.211	8.140	9.005	10.184
		R <sup>2</sup>	0.933	0.953	0.934	0.955	0.951
Ni-Cr/microcrystalline Cellulose	Langmuir	Qmax	129.870	102.041	101.010	95.238	93.458
		kL	0.037	0.065	0.080	0.108	0.138
		R <sup>2</sup>	0.827	0.937	0.957	0.945	0.961
	Freundlich	n	1.354	1.560	1.610	1.709	1.801
		kF	6.314	9.014	10.568	12.794	15.265
		R <sup>2</sup>	0.955	0.957	0.960	0.951	0.964

is close to one in the Freundlich isotherm model. Maximum adsorption capacity value (Qm) of ldh Ni-Cr/Cellulose composite adsorbent has the largest adsorption capacity of 129.870 mg/L. Langmuir isotherm adsorption process takes place in only a layer with a homogeneous surface, meanwhile, adsorption process with Freundlich isotherm happens in a heterogeneous surface (not uniform) of several layers so that it requires energy distribution (Kalam et al., 2021).

Looking at the data presented in Table 3, it can be concluded that the adsorption process of malachite green on Ni-Cr, microcrystalline cellulose, and Ni-Cr/microcrystalline cellulose adsorbents has a positive enthalpy value. Consecutively, the entropy values of the three ldhs with an initial concentration at 30 mg/L were 0.057 kJ/mol; 0.051 kJ/mol; and 0.075 kJ/mol. Along with the increase of temperature, the value of Gibbs energy is negative and getting smaller, it shows that the continuity of the reaction is spontaneous in the process of adsorption of malachite green on Ni-Cr, microcrystalline cellulose, and Ni-Cr/microcrystalline cellulose adsorbents.

**3.4 Analyze FT-IR (Fourier Transform-Infra Red) Characterization**

Based from FTIR investigations, it was observed that adsorption bands were formed, the adsorption intensity changed, and the intensity shifted. This suggests that the functional groups originated from the interaction between malachite green and the active sites of the adsorbents (chemical groups present in Ni-Cr LDH, microcrystalline cellulose, and Ni-Cr/microcrystalline cel-

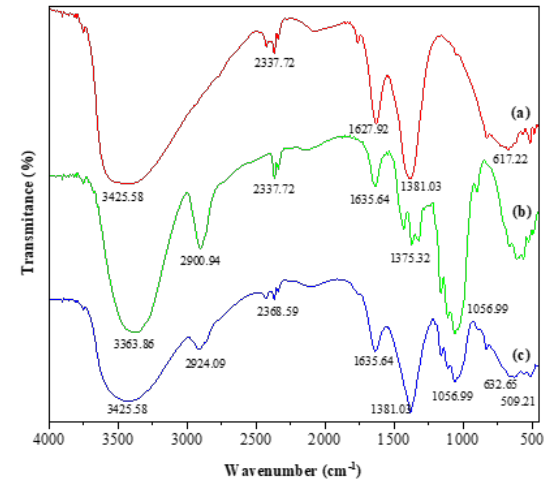


**Figure 6.** Spectrums FT-IR of Ni-Cr (a) Microcrystalline Cellulose (b) and Ni-Cr/microcrystalline Cellulose (c)

lulose LDH composites). The dye became bound to the active sites of the adsorbents through an electrostatic attraction mechanism. Figure 6(a) represents FTIR spectrum characterization of Ni-Cr LDH. FT-IR data shows there are vibrations at wavelengths of 3425.58; 2337.72; 1627.92; 1381.03; and 617.22 in units of cm<sup>-1</sup>. In the case of Siregar et al. (2021), the vibrations in the wave number range of 3440-3470 cm<sup>-1</sup> show that there is a hydroxy group (O-H). Vibrations under 1000 cm<sup>-1</sup> wave number range

**Table 3.** Thermodynamic Parameter for Removal Malachite Green Use Ni-Cr (a), Microcrystalline Cellulose (b), and Ni-Cr/microcrystalline Cellulose (c)

Concentration (mg/L)	T (K)	$\Delta H$ (kJ/mol)			$\Delta S$ (kJ/mol)			$\Delta G$ (kJ/mol)		
		a	b	c	a	b	c	a	b	c
30	303							-1.602	-2.366	-3.268
	313							-2.175	-2.874	-4.020
	323	15.748	13.031	19.510	0.057	0.051	0.075	-2.747	-3.382	-4.772
	333							-3.320	-3.890	-5.523
	343							-3.893	-4.399	-6.275
40	303							-1.808	-2.521	-3.226
	313							-2.317	-3.037	-4.020
	323	13.608	13.112	16.131	0.051	0.052	0.064	-2.826	-3.553	-4.772
	333							-3.335	-4.069	-5.523
	343							-3.843	-4.585	-6.275
50	303							-1.551	-2.272	-3.160
	313							-1.943	-2.640	-3.694
	323	10.345	8.875	13.004	0.039	0.037	0.053	-2.336	-3.008	-4.227
	333							-2.728	-3.376	-4.761
	343							-3.121	-3.744	-5.294
60	303							-1.528	-2.081	-3.050
	313							-1.920	-2.462	-3.627
	323	10.348	9.474	14.452	0.039	0.038	0.058	-2.312	-2.843	-4.205
	333							-2.704	-3.225	-4.782
	343							-3.096	-3.606	-5.360
70	303							-0.856	-1.483	-2.428
	313							-1.230	-1.866	-2.910
	323	10.460	10.111	12.168	0.037	0.038	0.048	-1.603	-2.248	-3.391
	333							-1.977	-2.631	-3.873
	343							-2.350	-3.013	-4.355

indicate the interaction between metal and oxygen (M-O), and in the 1610-1630  $\text{cm}^{-1}$  wave number range provide information that there are H<sub>2</sub>O groups. The anions present between layers of LDH can be seen from the peaks that appear in the infrared spectrum. The vibrations produced for each anion are not the same, such as the presence of nitrate ions at wave number 1384  $\text{cm}^{-1}$ .

Spectrum results of cellulose are presented in Figure 6(b). Wave numbers 1635.64 and 3363.86  $\text{cm}^{-1}$ , there is a widened absorption, indicating the presence of O-H stretching and bending groups. Stretching of the C=O group is obtained at wave numbers 2337.72  $\text{cm}^{-1}$ . Wave number 2900.94  $\text{cm}^{-1}$  there is a vibrational peak indicating the C-H group. Wave number 1056.99  $\text{cm}^{-1}$  indicates the C-O group. characteristic of microcrystalline cellulose is pyronose ring (C-O-C) found at wave number 1375.52  $\text{cm}^{-1}$ . Research conducted by Osman et al. (2022) shows the results of the cellulose spectrum, there is an O-H group at a wavelength of 3329  $\text{cm}^{-1}$ . There is a C-H group at a wavelength of 2890  $\text{cm}^{-1}$ , and C-O range from 1050-1150  $\text{cm}^{-1}$ . Glicosidic bonding found at wave number 900  $\text{cm}^{-1}$ . Figure 6(c) shows the results of the FTIR spectrum for the Ni-Cr/microcrystalline cellulose LDH

composite. Vibrations that appear at a wavelength of 3425.58  $\text{cm}^{-1}$  confirm that there is an O-H group. At a wavelength of 1635.64  $\text{cm}^{-1}$  shows that there is an H-O-H group. There is an absorption peak that indicates a C-O group at a wavelength of 2337.72  $\text{cm}^{-1}$ . Vibration at wave number 1627.92  $\text{cm}^{-1}$  there is a bending O-H group.  $\text{NO}_3^-$  group is present at a wavelength of 1381.03  $\text{cm}^{-1}$ . Yadav et al. (2018) have observed that modification of LDH with cellulose has the following FTIR spectrum results, which are O-H groups found at wave numbers in the range of 3350-3500  $\text{cm}^{-1}$ . M-O-H and M-O groups are found in the range of wave numbers 553, 682, 778, and 1364  $\text{cm}^{-1}$  and there are vibrational peaks found at wave numbers 1111, 1521, and 2321  $\text{cm}^{-1}$  which indicate the presence of C-O groups. Based on this research and the similarity of the vibrational peaks, the Ni-Cr/microcrystalline cellulose LDH composite compound was successfully synthesised.

### 3.5 Analyze SEM-EDX (Scanning Electron Microscopy- Energy Dispersive X-Ray) Characterization

Scanning Electron Microscopy (SEM) analysis has been performed to determine the morphology of the material and the

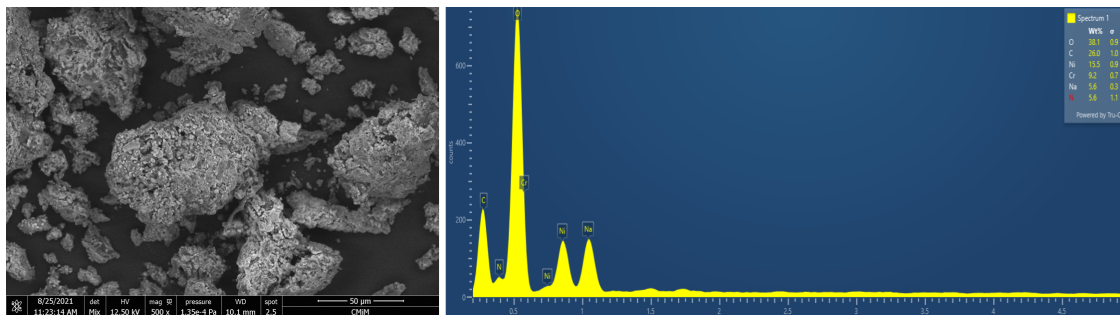


Figure 7. SEM-EDX Results of Ni-Cr/microcrystalline Cellulose

Table 4. EDX Data of Ni-Cr/microcrystalline Cellulose

Element	Chemical Composition Mass (%)
O	38.1
C	26.0
Ni	15.5
Cr	9.2
Na	5.6
N	5.6

particle size of the material by correlating it with the results of the adsorption process. Graph of particle distribution can be seen in Figure 7. Composite adsorbent can be seen to have an aggregate shape with a magnification of 500 $\times$  and has a particle size with the largest frequency of 1.954  $\mu\text{m}$  as many as 72. SEM image of Ni-Cr/microcrystalline cellulose shows that the structure of composite is porous and the surface is rough. This can be used as a support in adsorbing malachite green dye so as to increase the adsorption capacity due to the numerous pores in the composite material. Particle size can be calculated using ImageJ application and particle size produced can be correlated with functional groups. Large particle size can also affect the adsorption capacity of microcrystalline Ni-Cr/cellulose LDH composites (Çelebi et al., 2020).

EDX analysis can provide information about the atomic composition of the Ni-Cr/microcrystalline cellulose LDH composite material. Compound composition of Ni-Cr/microcrystalline cellulose LDH composite material is shown with the help of EDX (Energy Dispersive X-Ray) analysis in Table 4. The abundance of O elements contained in Ni-Cr/microcrystalline cellulose is also shown in FT-IR spectra that there is a wide band signifying O-H groups, and the presence of Ni and Cr metal elements in EDX supports the results of FT-IR spectrum data. EDX analysis results of the Ni-Cr/microcrystalline cellulose LDH composite consist of 38.1% oxygen and 26% carbon obtained from cellulose. Nickel 15.5%, and chrome 9.2% were obtained from Ni-Cr LDH. Sodium 5.6% was obtained from sodium hydroxide, and nitrogen 5.6% was obtained from impurities.

#### 4. CONCLUSIONS

Results of study of regeneration, Ni-Cr/microcrystalline cellulose LDH composite can be regenerated as much as five cycle and percent adsorbed until 51.873%. XRD characterization of Ni-Cr/microcrystalline cellulose LDH composite showed peaks at diffraction angles of 11°, 22.8°, 34.8°, and 60.3° which are typical regions of the Ni-Cr LDH and at diffraction angle of 22.67° which is a typical area of microcrystalline cellulose material. Adsorption process for optimum pH was found at pH 7 when there was no addition of  $\text{H}^+$  or  $\text{OH}^-$ . Optimum time for adsorption at 150 minutes. Pseudo second order adsorption kinetic is more suitable to explain the adsorption process. The parameter adsorption isotherm of malachite green dye on the three adsorbents leads to the Freundlich isotherm model with maximum adsorption capacity values in order 100.000; 104.167; 129.870 ( $\text{mg}\cdot\text{g}^{-1}$ ) and occurs endothermic which runs spontaneously. The results of the FTIR analysis show the specific vibrations of LDH at wave numbers 3425.58  $\text{cm}^{-1}$  (O-H), 617.22  $\text{cm}^{-1}$  (M-O), 1627.92  $\text{cm}^{-1}$  (H-O-H), and 1381.03  $\text{cm}^{-1}$  ( $\text{NO}_3^-$ ). Ni-Cr/microcrystalline cellulose LDH composite showed vibrations at wave numbers almost similar to LDH Ni-Cr and there are (C-C) 2900.94  $\text{cm}^{-1}$  and 1056.99  $\text{cm}^{-1}$  (C-O) groups which are adsorption from microcrystalline cellulose. SEM analysis showed that Ni-Cr/microcrystalline cellulose LDH composite has the properties of LDH particles in the form of irregular aggregates. From the EDX data, there are 38.1% oxygen, 26.0% carbon, 15.5% nickel, 9.2% chromium, 5.6% sodium, and 5.6% nitrogen.

#### 5. ACKNOWLEDGEMENT

The authors thank the Basecamp Team for fruitful discussions and comments on the research and manuscript.

#### REFERENCES

- Abid, M. F., M. A. Zablouk, and A. M. Abid-Alameer (2012). Experimental Study of Dye Removal from Industrial Wastewater by Membrane Technologies of Reverse Osmosis and Nanofiltration. *Iranian Journal of Environmental Health Science & Engineering*, 9; 1–9
- Adegoke, K. A. and O. S. Bello (2015). Dye Sequestration Using Agricultural Wastes as Adsorbents. *Water Resources and Industry*, 12; 8–24

- Ahmed, S. B., N. M. Mahmoud, A. A. Manda, and H. M. Refaat (2022). Study of the Optimization and Mechanism for the Remediation Process of Malachite Green Dye via Hybrid-based Magnetite-date's Stones. *Alexandria Engineering Journal*, **61**(12); 9879–9889
- Al-Tohamy, R., S. S. Ali, F. Li, K. M. Okasha, Y. A.-G. Mahmoud, T. Elsamahy, H. Jiao, Y. Fu, and J. Sun (2022). A Critical Review on the Treatment of Dye-containing Wastewater: Ecotoxicological and Health Concerns of Textile Dyes and Possible Remediation Approaches for Environmental Safety. *Ecotoxicology and Environmental Safety*, **231**; 113160
- Ashekuzzaman, S. and J.-Q. Jiang (2014). Study on the Sorption-Desorption-Regeneration Performance of Ca-, Mg-And CaMg-Based Layered Double Hydroxides for Removing Phosphate from Water. *Chemical Engineering Journal*, **246**; 97–105
- Ashraf, M. W., N. Abulibdeh, and A. Salam (2019). Selective Removal of Malachite Green Dye from Aqueous Solutions by Supported Liquid Membrane Technology. *International Journal of Environmental Research and Public Health*, **16**(18); 3484
- Ballav, N., R. Das, S. Giri, A. M. Muliwa, K. Pillay, and A. Maity (2018). L-cysteine Doped Polypyrrole (PPy@ L-Cyst): A Super Adsorbent for the Rapid Removal of Hg<sup>+2</sup> and Efficient Catalytic Activity of the Spent Adsorbent for Reuse. *Chemical Engineering Journal*, **345**; 621–630
- Celebi, H., G. Gök, and O. Gök (2020). Adsorption Capability of Brewed Tea Waste in Waters Containing Toxic Lead (II), Cadmium (II), Nickel (II), and Zinc (II) Heavy Metal Ions. *Scientific Reports*, **10**(1); 17570
- Chandanshive, V., S. Kadam, N. Rane, B.-H. Jeon, J. Jadhav, and S. Govindwar (2020). In Situ Textile Wastewater Treatment in High Rate Transpiration System Furrows Planted with Aquatic Macrophytes and Floating Phytobeds. *Chemosphere*, **252**; 126513
- Correcher, V. and J. García-Guinea (2018). Cathodo-and Photoluminescence Emission of a Natural Mg-Cr Carbonate Layered Double Hydroxide. *Applied Clay Science*, **161**; 127–131
- Dang, T., T. Mai, M. Truong, L. Dao, and T. Nguyen (2016). Optimization of the Photochemical Degradation of Textile Dye Industrial Wastewaters. *ASEAN Journal on Science and Technology for Development*, **33**(1); 10–17
- De Gisi, S., G. Lofrano, M. Grassi, and M. Notarnicola (2016). Characteristics and Adsorption Capacities of Low-Cost Sorbents for Wastewater Treatment: A Review. *Sustainable Materials and Technologies*, **9**; 10–40
- Dehbi, A., Y. Dehmani, H. Omari, A. Lammini, K. Elazhari, and A. Abdallaoui (2020). Hematite Iron Oxide Nanoparticles ( $\alpha$ -Fe<sub>2</sub>O<sub>3</sub>): Synthesis and Modelling Adsorption of Malachite Green. *Journal of Environmental Chemical Engineering*, **8**(1); 103394
- Doungmo, G., T. Kamgaing, R. C. T. Temgoua, E. Ymele, F. M. M. Tchieno, and I. K. Tonlé (2016). Intercalation of Oxalate Ions in the Interlayer Space of a Layered Double Hydroxide for Nickel Ions Adsorption. *International Journal of Basic and Applied Sciences*, **5**(2); 144
- Eltaweil, A., H. A. Mohamed, E. M. Abd El-Monaem, and G. El-Subruiti (2020). Mesoporous Magnetic Biochar Composite for Enhanced Adsorption of Malachite Green Dye: Characterization, Adsorption Kinetics, Thermodynamics and Isotherms. *Advanced Powder Technology*, **31**(3); 1253–1263
- Fouad, H., L. K. Kian, M. Jawaid, M. D. Alotaibi, O. Y. Alothman, and M. Hashem (2020). Characterization of Microcrystalline Cellulose Isolated from Conocarpus Fiber. *Polymers*, **12**(12); 2926
- Gomes, A., D. Cocke, D. Tran, and A. Baksi (2016). Layered Double Hydroxides in Energy Research: Advantages and Challenges. *Energy Technology 2015: Carbon Dioxide Management and other Technologies*; 309–316
- Guo, X. and J. Wang (2019). A General Kinetic Model for Adsorption: Theoretical Analysis and Modeling. *Journal of Molecular Liquids*, **288**; 111100
- Hamad, H. and M. T. Moustafa (2023). Optimization Study of the Adsorption of Malachite Green Removal by MgO Nano-Composite, Nano-Bentonite and Fungal Immobilization on Active Carbon Using Response Surface Methodology and Kinetic Study. *Environmental Sciences Europe*, **35**(1); 1–37
- Jiang, Z., F. Sun, R. L. Frost, G. Ayoko, G. Qian, and X. Ruan (2022). Adsorption Characteristics of Assembled and Unassembled Ni/Cr Layered Double Hydroxides Towards Methyl Orange. *Journal of Colloid and Interface Science*, **617**; 363–371
- Kalam, S., S. A. Abu-Khamsin, M. S. Kamal, and S. Patil (2021). Surfactant Adsorption Isotherms: A Review. *ACS Omega*, **6**(48); 32342–32348
- Karam, A., E. S. Bakhroum, and K. Zaher (2021). Coagulation/flocculation Process for Textile Mill Effluent Treatment: Experimental and Numerical Perspectives. *International Journal of Sustainable Engineering*, **14**(5); 983–995
- Katheresan, V., J. Kannedo, and S. Y. Lau (2018). Efficiency of Various Recent Wastewater Dye Removal Methods: A Review. *Journal of Environmental Chemical Engineering*, **6**(4); 4676–4697
- Matpang, P., M. Sriuttha, and N. Piwpuan (2017). Effects of Malachite Green on Growth and Tissue Accumulation in Pak Choy (*Brassica chinensis* Tsen & Lee). *Agriculture and Natural Resources*, **51**(2); 96–102
- Medidi, S., S. Markapurapu, M. R. Kotupalli, R. K. R. Chinnam, V. M. Susarla, H. B. Gandham, and P. D. Sanasi (2018). Visible Light Photocatalytic Degradation of Methylene Blue and Malachite Green Dyes with Cu<sub>2</sub>O-4-Go Nano Composite. *Modern Research in Catalysis*, **7**(2); 17–34
- Muinde, V. M., J. M. Onyari, B. Wamalwa, and J. N. Wabomba (2020). Adsorption of Malachite Green Dye from Aqueous Solutions Using Mesoporous Chitosan-Zinc Oxide Composite Material. *Environmental Chemistry and Ecotoxicology*, **2**; 115–125
- Nandoost, A., N. Bahramifar, A. A. Moghadamnia, S. Kazemi (2022). Adsorption of Malachite Green (MG) as a Cationic Dye on Amberlyst 15, an Ion-Exchange Resin. *Journal of Environmental and Public Health*, **2022**; 4593835
- Normah, N. R. Palapa, T. Taher, R. Mohadi, F. S. Arsyad, A. Pri-

- ambodo, A. Lesbani (2021). Competitive Removal of Cationic Dye using NiAl-LDH Modified with Hydrochar. *Ecological Engineering & Environmental Technology*, **22**(4); 124–135
- Olisah, C., J. B. Adams, and G. Rubidge (2021). The State of Persistent Organic Pollutants in South African Estuaries: A Review of Environmental Exposure and Sources. *Ecotoxicology and Environmental Safety*, **219**; 112316
- Osman, A. I., S. Fawzy, C. Farrell, H. Ala'a, J. Harrison, S. Al-Mawali, and D. W. Rooney (2022). Comprehensive Thermokinetic Modelling and Predictions of Cellulose Decomposition in Isothermal, Non-Isothermal, and Stepwise Heating Modes. *Journal of Analytical and Applied Pyrolysis*, **161**; 105427
- Palapa, N. R., A. F. Badri, R. Mohadi, T. Taher, and A. Lesbani (2022). Mg/Cr-(COO) 22-layered Double Hydroxide for Malachite Green Removal. *Communications in Science and Technology*, **7**(1); 91–97
- Ruan, X., Y. Chen, H. Chen, G. Qian, and R. L. Frost (2016). Sorption Behavior of Methyl Orange from Aqueous Solution on Organic Matter and Reduced Graphene Oxides Modified Ni–Cr Layered Double Hydroxides. *Chemical Engineering Journal*, **297**; 295–303
- Sarro, M., N. P. Gule, E. Laurenti, R. Gamberini, M. C. Paganini, P. E. Mallon, and P. Calza (2018). ZnO-Based Materials and Enzymes Hybrid Systems as Highly Efficient Catalysts for Recalcitrant Pollutants Abatement. *Chemical Engineering Journal*, **334**; 2530–2538
- Sartape, A. S., A. M. Mandhare, V. V. Jadhav, P. D. Raut, M. A. Anuse, and S. S. Kolekar (2017). Removal of Malachite Green Dye from Aqueous Solution with Adsorption Technique Using Limonia Acidissima (Wood Apple) Shell as Low Cost Adsorbent. *Arabian Journal of Chemistry*, **10**; S3229–S3238
- Silva, A. C., A. J. Silvestre, C. S. Freire, and C. Vilela (2021). Modification of Textiles for Functional Applications. *Fundamentals of Natural Fibres and Textiles*; 303–365
- Sinha, R. and R. Jindal (2018). Malachite Green Induced Acute Toxicity in Cyprinus Carpio. *Journal of Global Biosciences*, **7**(2); 5369–5374
- Siregar, P. M. S. B. N., N. R. Palapa, A. Wijaya, E. S. Fitri, and A. Lesbani (2021). Structural Stability of Ni/Al Layered Double Hydroxide Supported on Graphite and Biochar Toward Adsorption of Congo Red. *Science and Technology Indonesia*, **6**(2); 85–95
- Taher, T., Y. Irianty, R. Mohadi, M. Said, R. Andreas, and A. Lesbani (2019). Adsorption of Cadmium (II) Using Ca/Al Layered Double Hydroxides Intercalated with Keggin Ion. *Indonesian Journal of Chemistry*, **19**(4); 873–881
- Tang, L., J. Yu, Y. Pang, G. Zeng, Y. Deng, J. Wang, X. Ren, S. Ye, B. Peng, and H. Feng (2018). Sustainable Efficient Adsorbent: Alkali-Acid Modified Magnetic Biochar Derived from Sewage Sludge for Aqueous Organic Contaminant Removal. *Chemical Engineering Journal*, **336**; 160–169
- Venkatesh, S., K. Venkatesh, and A. R. Quaff (2017). Dye Decomposition by Combined Ozonation and Anaerobic Treatment: Cost Effective Technology. *Journal of Applied Research and Technology*, **15**(4); 340–345
- Yadav, A., M. Pal, and R. L. Goswamee (2018). Biocompatible Nanocomposite of Carboxymethyl Cellulose and Functionalized Carbon–Norfloxacin Intercalated Layered Double Hydroxides. *Carbohydrate Polymers*, **186**; 282–289
- Yuliasari, N., A. Wijaya, R. Mohadi, and A. Lesbani (2023). Enhanced Effectiveness on Phenol Removal by MgCr-LDH/Microcrystalline Cellulose Composite and Regeneration Study with Green Desorption Reagent. *Science and Technology Indonesia*, **8**(1); 151–159